Desalination and Water Treatment
www.deswater.com
doi: 10.5004/dwt.2019.24274

158 (2019) 207–215
August

Simultaneous adsorption of heavy metal ions (Cu^{2+} and Cd^{2+}) from aqueous solutions by magnetic silica nanoparticles (Fe_3O_4@SiO_2) modified using EDTA

Ali Esrafili, Samaneh Bagheri*, Majid Kermani, Mitra Gholami, Mehrdad Moslemzadeh

Research Center for Environmental Health Technology, Iran University of Medical Sciences, Iran, Tel. +98 9333110705; email: samanebagheri67@gmail.com (S. Bagheri), Tel. +98 9124976672; Fax: +98 2188607939; email: a_esrafily@yahoo.com (A. Esrafily), Tel. +98 9122250387; email: majidkermani@yahoo.com (M. Kermani), Tel. +98 9123906308; email: gholamim@iums.ac.ir (M. Gholami), Tel. +98 9116075024; email: mehrdad.moslemzadh@gmail.com (M. Moslemzadeh)

Received 26 October 2018; Accepted 12 April 2019

ABSTRACT

In this study, Fe_3O_4@SiO_2 magnetic nanoparticles are modified with EDTA and used as a selective and efficient adsorbent for the removal of Cu^{2+} and Cd^{2+} heavy metals. The Fe_3O_4@SiO_2-EDTA nano composite is characterized using scanning electron microscopy, energy-dispersive X-ray, X-ray diffraction, Fourier-transform infrared spectroscopy, and Brunauer–Emmett–Teller. Nanoparticles are separated by an external magnet after the adsorption process. Adsorption equilibrium is achieved in 60 min, and the maximum removal of metal ions is obtained at pH 7. Isotherm analysis indicated that the adsorption data fit well to the Langmuir isotherm model. The maximum adsorption capacities are 79.4 and 73.5 mg/g for Cu^{2+} and Cd^{2+}, respectively. In addition, adsorption kinetic data agree with pseudo-second-kinetic order for both tested metal ions. Also, the adsorption process efficiency is investigated in the presence of K^+, Na^+, Mg^{2+}, and Ca^{2+} cations at the optimal conditions. This study indicates that the Fe_3O_4@SiO_2-EDTA is a rapid, efficient, and reusable sorbent to remove Cd^{2+} and Cu^{2+} cations from contaminated aquatic solution.

Keywords: Fe_3O_4@SiO_2; Fe_3O_4@SiO_2-EDTA; Cu^{2+}; Cd^{2+}

1. Introduction

One of the greatest environmental concerns is the pollution of water resources by toxic organic compounds and heavy metals. Such contaminants originate from industrial development, which has increased wastewater production, and emission of pollutants, especially heavy metals, to aqueous environments [1]. Heavy metals receive major consideration because of their persistent toxic effect and their ability to accumulate within compartments of the environment. They are either of natural origin or from anthropogenic activities. Anthropogenic activities, which are primary sources of heavy metal pollution, including mineral resources development, metal processing and smelting, chemical production, factory emissions, and sewage irrigation [2]. However, the most hazardous heavy metals for living species are arsenic (As), cadmium (Cd), chromium (Cr), lead (Pb), copper (Cu), and mercury (Hg) [3,4]. These metals can penetrate living tissues, which results in damaging them, even in low quantities. Presence of these metals in drinking water, even in little amounts, can cause harmful effects on the central nervous system, kidneys, skin, teeth, liver, or lungs. Long-term exposure to larger amounts may even lead to death [3]. Two of the most important examples of these heavy metals are Cu and Cd. The current maximum containment levels for Cu and Cd in drinking water are, respectively, 1.3 and 0.005 mg/L [5]. In conclusion, water contaminated by these

* Corresponding author.

heavy metals should be treated before discharging into water resources.

Conventional methods for the removal of heavy metals from aqueous solutions include ion exchange, membrane process, chemical precipitation, reverse osmosis, solvent-based extraction, and adsorption [3,6,7]. Most of these processes have problems such as high-cost, high amount of sludge, sludge disposal, and high energy consumption [8]. Among these processes, adsorption is considered to be an effective technique for water and wastewater treatment. This is because of its simplicity, applicability, cost-effectiveness, insensitivity to pollutants, lack of toxic compound formation, adsorbent, and the possibility of reusing the adsorbate [8]. Specifically, adsorption of metals by eco-friendly nanoparticles (NPs) has attracted much interest as an efficient technique for the removal of organic contaminants and heavy metal ions from water and wastewater [7]. In recent years, the nanoparticles have been used to remove pollutants as adsorption processes [9–11], and as heterogeneous advanced oxidation processes [12,13].

Adsorbent NPs are usually modified by different materials to enhance their physical and chemical properties. Silica (SiO_2), for instance, has been widely used to improve dispersibility and chemical stability of iron oxide NPs in aqueous mediums [3,14,15]. Coating iron oxide cores by neutral silica can provide hydrophobicity, environment friendliness and a higher surface area for adsorption of the target adsorbates, especially heavy metals [14]. Also, deposition of SiO_2 on iron oxide NPs can lead to structural stability. However, when they are coated by SiO_2 layers, their resistance is promoted against structural changes. That is why conservation of crystalline structure plays an important role in the final properties of iron oxide-based composites [16]. Furthermore, silica layers prevent dissolution of iron oxide NPs under acidic conditions. Another advantage of applying SiO_2 coatings is that they can be chemically modified by the addition of different functional groups to improve removal efficiency by iron oxide NPs. In other words, the advantages of SiO_2 are accessibility, high surface area (about 600 m^2/g), and high thermal resistance, which can lead to removal of Pb^{2+}, Cd^{2+}, Fe^{2+}, Zn^{2+}, Cu^{2+}, and Mn^{2+} from contaminated waters [3,17].

Even though SiO_2 layers are so advantageous for adsorption purposes, they cannot act reversibly in adsorption of metals [18]. Hence, recovery of adsorbent particles would be complicated. This can be solved through functionalizing silica layers by different organic compounds, for example, ethylene diamine tetra acetic acid (EDTA) [15]. In case of iron oxide NPs, chemical modifications by using chelating agents, such as EDTA, can help advancement of strong interactions with metal ions, improvement of adsorption capacity, and shortening equilibration time. In optimum conditions, modified adsorbent with EDTA can be used as a selective and effective adsorbent for removal of various heavy metals [19]. In this study, the EDTA chelating agent is investigated as an effective modifier for adsorption of Cu^{2+} and Cd^{2+} ions in contaminated water. Hence, the aim of this study is to investigate the potential of EDTA adsorption onto the Fe_3SO_4@ SiO_2 nanoparticles to remove Cu^{2+} and Cd^{2+} ions from aqueous solution.

2. Materials and methods

2.1. Experimental setup

2.1.1. Instrumentation and chemicals

$FeCl_2{\cdot}4H_2O$ and $FeCl_3{\cdot}6H_2O$, tetraethoxysilane (TEOS), cadmium nitrate tetrahydrate ($Cd(NO_3)_2{\cdot}4H_2O$), copper nitrate trihydrate ($Cu(NO_3)_2{\cdot}3H_2O$), toluene and ethanol (>99.5%), acetic acid (>99.7%), ammonia, nitric acid, hydrochloric acid, sodium hydroxide, and sulfuric acid are purchased from Sigma-Aldrich Chemical Company (Germany). EDTA is purchased from ABCR Chemical Company (Germany). All solutions are prepared using deionized water.

2.1.2. Preparation of magnetite Fe_3O_4 nanoparticles

To be more specific, 11.4 g of $FeCl_3{\cdot}6H_2O$ and 4.1 g of $FeCl_2{\cdot}4H_2O$ are dissolved in distilled water into a beaker. First, the ferrous ion solution is transferred to a reactor, and its volume has reached to 400 mL. Then, the temperature of the reactor is adjusted to 80°C, and its contents are mixed for 1 h at 600 rpm under a nitrogen atmosphere to exclude any dissolved oxygen molecules from the reactor. After that, a solution of 0.25% ammonia is added to the reactor. At this point, the brown solution has turned black. After completion of the reaction, a portion of the resultant mixture is poured into a 100 mL beaker. Reassuring the quality of magnetic NPs, a magnet is placed beside the beaker. Movement of the particles toward the magnet will approve the completion of the reaction [7].

2.1.3. Synthesis of Fe_3O_4@SiO_2

The prepared Fe_3O_4 NPs were coated with SiO_2. For this purpose, the magnetic NPs are dispersed in 20 mL TEOS, 6 mL ammonia (28%), 80 mL ethanol (65%), and deionized water into 250 mL beaker. The resulted suspension is injected into the reactor dropwise. The reactor contents are stirred at 600 rpm. Then, the particles are separated using a magnet, washed with ethanol and distilled water for a few times and dried at 60°C in an oven [20]. This process resulted in producing Fe_3O_4@SiO_2 NPs.

2.1.4. Fe_3O_4@SiO_2 functionalization by EDTA

10 mL of EDTA is diluted in methanol and distilled water, and added to the Fe_3O_4@SiO_2 NPs at 80°C. After 72 h, the resulted NPs are washed with distilled water and dried at room temperature [16].

2.2. Adsorbent characterization

The Fe_3O_4@SiO_2-EDTA beads are characterized using scanning electron microscopy (SEM), energy-dispersive X-ray (EDX), Brunauer–Emmett–Teller (BET), and X-ray diffraction (XRD) analyses. The formation of additional functional groups on Fe_3O_4 surface is studied by Fourier-transform infrared spectroscopy (FTIR) analysis (FTIR, AVA TAR370, NICOLET, USA) with KBr pellets.

2.3. Adsorption experiments

The adsorption process is carried out at ambient temperature (25°C), and conducted as one factor at a time. In the study, parameters of pH solution (2–9), contact time, initial Cu^{2+} and Cd^{2+} concentration (2–20 mg/L) and adsorbent dose (0.01–1 g/L) are as variations. The experiment is initiated with making stock solution of heavy metal followed by determining equilibrium time and optimizing one of the influenced parameters in the adsorption of Cu^{2+} and Cd^{2+} onto the Fe_3O_4@SiO_2-EDTA. At the end of each experiment, the Fe_3O_4@SiO_2-EDTA is separated by an external magnet (1.3 T) and the remained Cu^{2+} and Cd^{2+} concentrations are determined using a Shimadzu atomic adsorption AA-680 spectroscopy (made in Japan).

Metal ions removal efficiency and sorption capacity are calculated using Eqs. (1) and (2):

$$\text{Removal efficiency} = \frac{C_0 - C_t}{C_0} \times 100\% \quad (1)$$

$$\text{Sorption capacity} = q_e = \frac{\left(C_0 - C_t\right)}{m} \times V \quad (2)$$

where C_0 and C_t are the initial and final concentrations of metal ions (mg/L), m is the mass of nanoparticles (g), and V is the volume of solution (L).

Recovery efficiency is calculated using Eq. (3):

$$\text{Recovery effiency} = \frac{C_w}{C_0} \times 100 \quad (3)$$

where C_0 (mg/L) is the initial concentrations of metal ions and C_w (mg/L) is the concentration of metal ions in the extracted solution (after regeneration).

2.4. Adsorption isotherms

The Cd^{2+} and Cu^{2+} equilibrium adsorption is evaluated using the Langmuir and Freundlich isotherms model.

Langmuir isotherm model: the model states that the distribution of adsorbed solute is mono-layer with a homogeneous pattern over the active sites on the surface of the adsorbate. According to this model, the energy of adsorption is constant throughout the adsorption process, and its linear model as represented by Eq. (4):

$$\frac{C_e}{q_e} = \frac{1}{K_L \times q_m} + \frac{C_e}{q_m} \quad (4)$$

where C_e is the solute concentration (mg/L) at equilibrium, q_e is the amount adsorbed (mg/g), q_m is the maximum sorption capacity (mg/g), and K_L is energy of adsorption (L/mg) [21]. Note that

$$\log q_e = \log K_F + \frac{1}{n} \log C_e \quad (5)$$

where K_F and n are the extent of adsorption (mg/g) and adsorption intensity of system, respectively.

2.5. Adsorption kinetics

Kinetics is analyzed using the pseudo-first-order and pseudo-second-order models [22] using Eqs. (6) and (7);

$$\ln\left(q_e - q_t\right) = \ln\left(q_e\right) - k_1 t \quad (6)$$

$$\frac{t}{q_e} = \frac{1}{k_2 q_e^2} + \frac{1}{q_e} \times t \quad (7)$$

where k_1 (h^{-1}) and k_2 (g/mg/h) are the equilibrium rate constants of kinetics.

2.6. Regeneration and reuse of Fe_3O_4@SiO_2-EDTA

To investigate the regeneration and reuse of Fe_3O_4@SiO_2-EDTA, 10 mg/L of Cd^{2+} and Cu^{2+} solution is used with the same adsorption process followed by separation of the nano-adsorbent from solution with the handheld magnet. The Fe_3O_4@SiO_2-EDTA is collected and then washed with 1% HCl solution (10 min at the room temperature). The regenerated Fe_3O_4@SiO_2-EDTA particles are reused for subsequent $Cd^{2+}$and Cu^{2+} sorption experiments. The sorption, extraction, and reuse processes are repeated five times. Changes in sorption capacity and nanoparticles recovery are determined at every cycle [23].

2.7. pH at point zero charge

To determine pH at point zero charge (pH_{zpc}) for Fe_3O_4@SiO_2-EDTA particles, the following steps are performed. In the first step, a sufficient amount of 0.1 M $NaNO_3$ solution is poured into 250 mL flasks and the pH is adjusted in the range of 2–11 by either 1 M HCl or NaOH. In the second step, the whole volume of the solution in each flask is adjusted to 100 mL by adding $NaNO_3$ solution of the same concentration. At the same time, the initial pH values of the solutions are accurately noted. In the next step, 0.15 g of the NPs are added to the flasks and the suspensions are shaken and allowed to equilibrate for 24 h by a shaker. In the final step, the final pH values of the supernatant liquids containing NPs were noted [24].

3. Results and discussion

3.1. Characterization of adsorbent

The SEM images of the Fe_3O_4@SiO_2 and Fe_3O_4@SiO_2-EDTA particles are shown in Figs. 1a and b. Also, the results of EDX analysis for Fe_3O_4@SiO_2 and Fe_3O_4@SiO_2-EDTA are prepared in Table 1. According to these data, the functional groups are well distributed on the surface of the silica layer. Moreover, the Fe_3O_4@SiO_2 particle is composed of Fe, C, O, and Si while the data related to the Fe_3O_4@SiO_2-EDTA highlight the presence of Na in addition to these elements. This finding indicates successful introduction of the tetra acetic acid functional group to the Fe_3O_4@SiO_2 particles and formation of the Fe_3O_4@SiO_2-EDTA.

The XRD patterns of the Fe_3O_4@SiO_2 and Fe_3O_4@SiO_2-EDTA particles are presented in Fig. 2. The XRD patterns

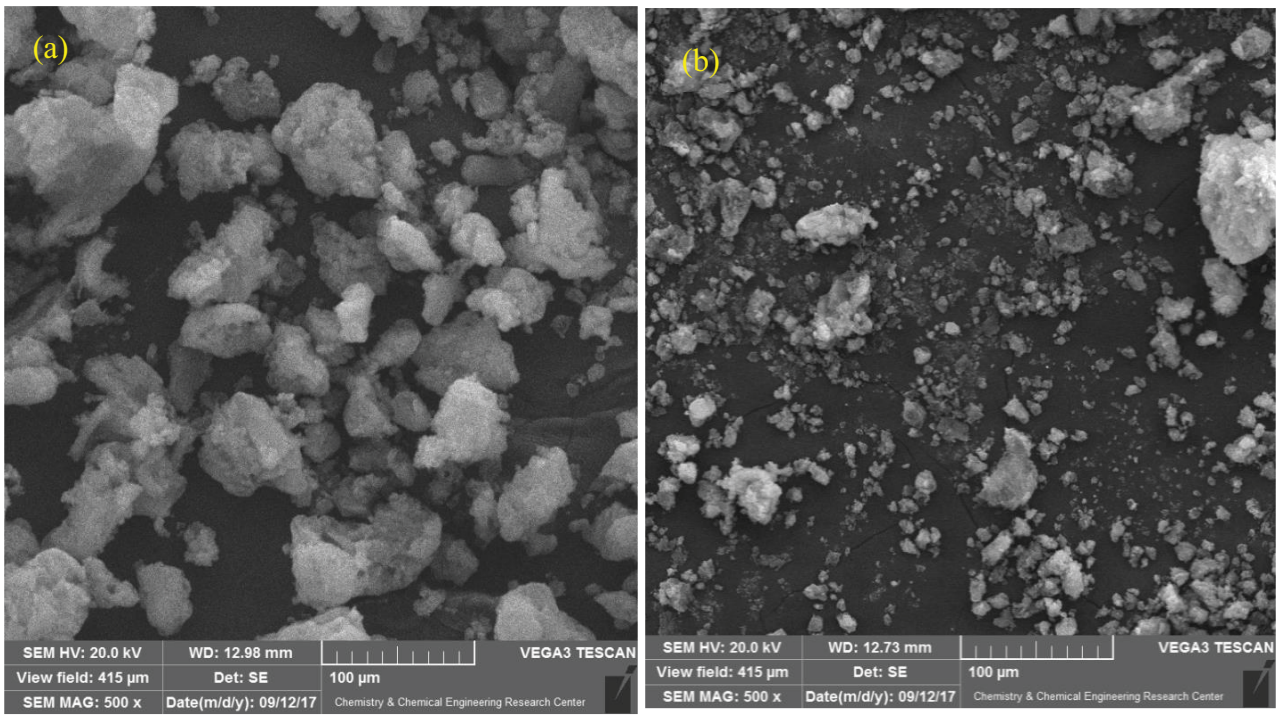

Fig. 1. SEM images of Fe_3O_4@SiO_2 (a) and Fe_3O_4@SiO_2-EDTA (b).

Table 1
EDX results of Fe_3O_4@SiO_2 and Fe_3O_4@SiO_2-EDTA

Fe_3O_4@SiO_2			Fe_3O_4@SiO_2-EDTA		
ELM	W%	A%	ELM	W%	A%
C	2.86	8.77	C	8.03	21.54
O	12.42	28.61	O	13.48	27.14
Si	10.35	13.57	Na	0.87	1.22
Fe	74.37	49.06	Si	9.34	10.71
			Fe	68.28	39.39

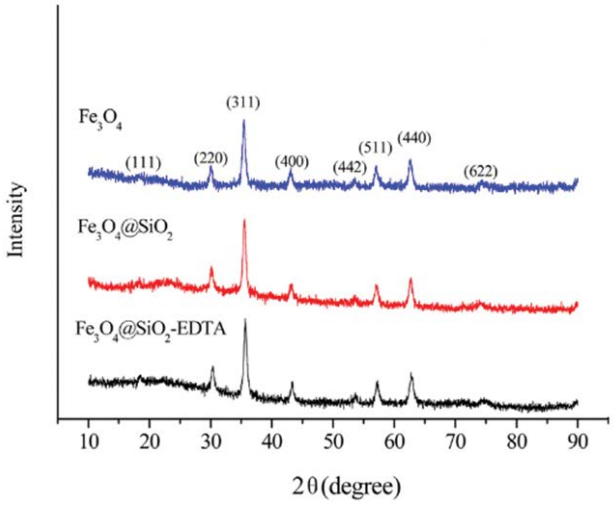

Fig. 2. XRD patterns of Fe_3O_4@SiO_2-EDTA.

show the position and relative intensities of all peaks for Fe_3O_4 at 18.27 (111), 30.07 (220), 35.44 (311), 43.06 (400), 53.4 (442), 56.95 (511), 62.51 (440), and 74.95 (622), confirming that pore Fe_3O_4 is cubic spinel structure [16]. No more peaks are assigned to the crystalline form in Fe_3O_4@SiO_2 and Fe_3O_4@SiO_2-EDTA (Fig. 2), and all of the diffraction peaks are indexed as the face centered cubic phases of Fe implying that modified Fe_3O_4 with EDTA retained the crystalline cubic spinel structure.

Specific surface areas are commonly treated according to the BET theory as a standard procedure to nitrogen adsorption/desorption isotherms measured at 77 K. The specific surface area of the sample is determined by physical adsorption of a gas on the surface of the solid and by measuring the amount of adsorbed gas corresponding to a monomolecular layer on the surface [3]. The results of the BET method show that the average specific surface areas of Fe_3O_4 and Fe_3O_4@SiO_2 are 42.3 and 70.8 m^2/g, respectively. However, after functionalizing the surface of Fe_3O_4@SiO_2 nanoparticles with EDTA, the specific surface area of Fe_3O_4@SiO_2-EDTA is decreased to 24.1 m^2/g. It should be noted that the decrease in surface area may be resulted from the increase in the size of particles and the agglomeration of particles. Also, the pore size and the total pore volume of Fe_3O_4@SiO_2 are determined to be 9.2 nm and 3.6×10^{-3} cm^3/g, respectively. The pore size and the total pore volume of Fe_3O_4@SiO_2-EDTA are 8.3 nm and 2.2×10^{-3} cm^3/g, respectively.

3.2. FTIR analysis

FTIR analysis of the Fe_3O_4, Fe_3O_4@SiO_2, and Fe_3O_4@SiO_2-EDTA is used to identify the type of functional groups on

the adsorbents. As shown in Fig. 3, for Fe_3O_4@SiO_2-EDTA the typical adsorption peaks at 456 and 590 cm^{-1} are attributed to the stretching vibration of Fe–O bond. The presence of a peak at 3,416 cm^{-1} is ascribed to the –OH stretching. The peak at 1,084 cm^{-1} is related to Si–O–C and symmetric Si–O–Si stretching vibrations, and the peak at 798 cm^{-1} is related to Si–OH, implying the successful formation of silica layers on Fe_3O_4. Moreover, the strong characteristic adsorption band appeared at 1,635 cm^{-1} assigned to the stretching vibration of C=O in symmetrical –COOH groups, while this peak could be also assigned to C–N bond and γ_{CH2} group. All these peaks are in Fe_3O_4@SiO_2 spectrum. After bonding EDTA to Fe_3O_4@SiO_2, an enhanced adsorption peak at 1,734 cm^{-1} is assigned to the C=O stretching vibrations of the asymmetrical COO^- [16]. These bands indicate the formation of carboxylic on the Fe_3O_4, and show that the synthesis procedure is successfully assembled EDTA on the surface of magnetite nanoparticles [23,25].

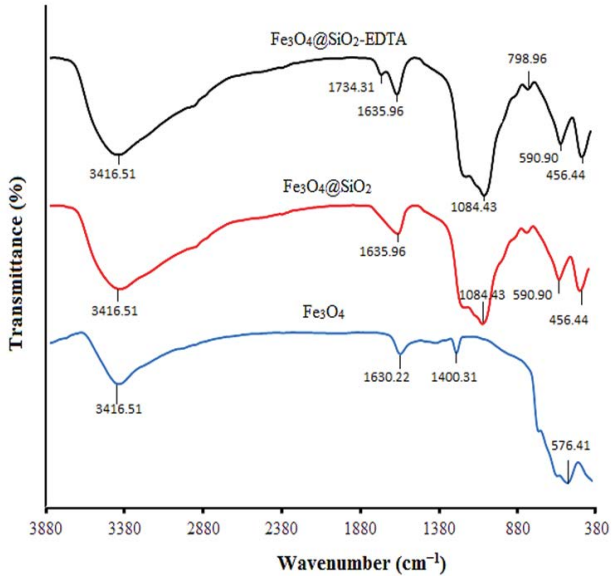

Fig. 3. Fourier-transform infrared analysis of Fe_3O_4@SiO_2-EDTA.

3.3. Effect of pH on Cu^{2+} and Cd^{2+} adsorption

One of the important parameters which affects the adsorption processes is pH solution value. This value influences the concentration of cationic species. Depending on pH, metal ions can be cationic or form metal hydroxides and precipitate [26]. As shown in Fig. 4, increasing pH from 3 to 7 increases the removal efficiency of Cu^{2+} and Cd^{2+} while further increase of pH from 8 to 9 decreases the removal efficiency. The pH_{zpc} for Fe_3O_4@SiO_2-EDTA NPs is 5.0, as shown in Fig. 4a. At pH values higher than the pH_{zpc}, the NPs surface charge is negative, and by increasing pH, the negative charge on the NPs surface increases [8]. Therefore, the adsorption of Cu^{2+} and Cd^{2+} cations onto the Fe_3O_4@SiO_2-EDTA NPs increases by pH = 7.0. Also, the low adsorption removal of the metal ions at acidic conditions (pH < 7) can be attributed to the intense competition of the H^+ ions with Cu^{2+} and Cd^{2+} for adsorption onto the active sites. In fact, adsorption of H^+ onto the active sites can cause electrostatic repulsion between the positive metal ions and the positive surface of the adsorbent and reduce metal ion adsorption [11]. On the other hand, at basic conditions (pH > 7), a limited number of the Cu^{2+} and Cd^{2+} cations exist in the solution and most Cu^{2+} and Cd^{2+} metal ions convert to their metal hydroxides and precipitate. At the end, the adsorption efficiency increases due to the compression and precipitation of hydroxide ions (OH^-). The extent of adsorption depends on the type of the metal ion, and the adsorption percentage of Cd^{2+} is more than that of Cu^{2+} ions [16,27].

3.4. Effect of the adsorbent dosage

To investigate the effect of the adsorbent dosage on the adsorption efficiency of Cu^2 and Cd^{2+}, different amounts of adsorbent are added into the aqueous solution where Cu^2 and Cd^{2+} concentration and pH are 50 mg/L and 7, respectively. The results are presented in Fig. 5. The increase in adsorbent

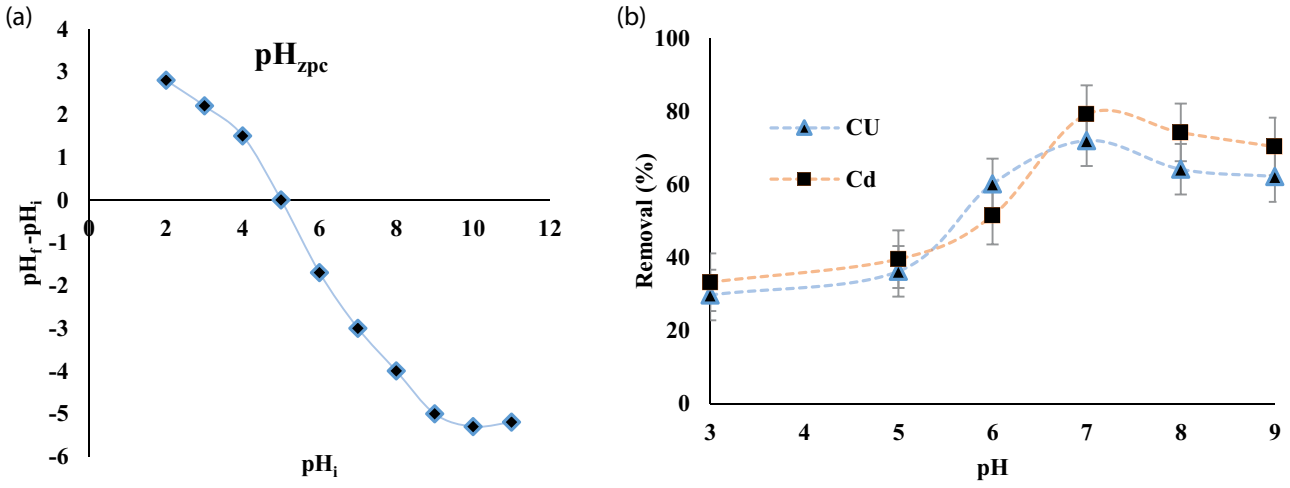

Fig. 4. pH evaluation results. The point of zero charge (a), and effect of pH on the removal of heavy metals by Fe_3O_4@SiO_2-EDTA nanoparticles in 120 min Cu^{2+} and Cd^{2+} (5 mg/L), adsorbent dose (0.3 g) (b).

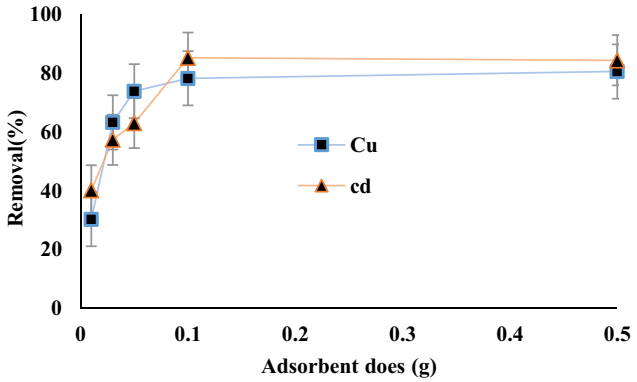

Fig. 5. Effect of the adsorbent dosage on the adsorption efficiency of Cu^{2+} and Cd^{2+}

dose, from 1.0 to 5.0 g, increases the removal efficiency of adsorbents. The reason is related to the increased number of active sites and promoted access of the two adsorbates to the adsorbent's surface, which enhance the possibility of adsorbate–adsorbent collisions and ion adsorption [25]. Similar results have been reported in other studies. For example, increasing adsorbent dose by 0.2 mg/L for Cd^{2+}, and 0.125 g/L for Pb^{2+} improves their removal efficiencies to over 97% [28].

3.5. Effect of contact time and initial Cu^{2+} and Cd^{2+} concentration

The effects of contact time on the removal of Cu^{2+} and Cd^{2+} by the Fe_3O_4@SiO_2-EDTA are shown in Fig. 6. The adsorption of metal ions increases with the increase in contact time and attained equilibrium within 60 min. Rapid increase of adsorption capacity at the initial stage of the process is due to the high access of the Cu^{2+} and Cd^{2+} ions to the unsaturated sites positioned on the surface of the Fe_3O_4@SiO_2-EDTA nanoparticles [21]. As the process continues, the sites get occupied, the ions gradually lose access to the sites, and finally the adsorption reaction equilibrates at a specific time. In other words, equilibration of the adsorption reaction happens when the concentration of the adsorbate in the solution phase be in dynamic equilibrium with its concentration at the solid–liquid interface [15]. The effect of initial concentration on the metal ions removal is studied in the concentration range from 2 to 20 mg/l, as shown in Fig. 6. The removal efficiency of Cu^{2+} and Cd^{2+} is increased with the increase in initial metal concentration. This increase in the removal efficiency can be explained with the high driving force for mass transfer over the adsorption process [23,28].

3.6. Adsorption kinetics

The adsorption of Cu^{2+} and Cd^{2+} onto the Fe_3O_4@SiO_2-EDTA involves the coordination of these metal ions by oxygen and nitrogen atoms, whose free electrons favor the formation of metal–adsorbent complexes onto the adsorbent surface. The rate at which the metal ions are transferred from the solution to the adsorbent surface determines the rate of the adsorption kinetics [27]. Table 2 depicts the adsorption kinetics of Cu^{2+} and Cd^{2+} onto the Fe_3O_4@SiO_2-EDTA as a function of time. Initial concentration is 10 mg/L, and the adsorption equilibrium is reached in approximately 60 min. This indicates that the adsorption takes place once contacting between the adsorbates and the adsorbent. The findings indicate that adsorption of Cu^{2+} and Cd^{2+} onto the Fe_3O_4@SiO_2-EDTA follows the pseudo-second-order kinetic model.

Table 2
Adsorption kinetic data for the removal of Cu^{+2} and Cd^{+2} onto Fe_3O_4@SiO_2-EDTA

Model	Parameter	Cd^{+2}	Cu^{+2}
Pseudo-first-order model	q_e (mg/g)	2.856	2.478
	K_1	0.0128	0.0012
	R^2	0.9664	0.923
	$q_{e\,(exp)}$	8.4	5.863
Pseudo-second-order model	q_e (mg/g)	4.0485	6.7526
	K_2	0.0254	0.0199
	R^2	0.9993	0.9997

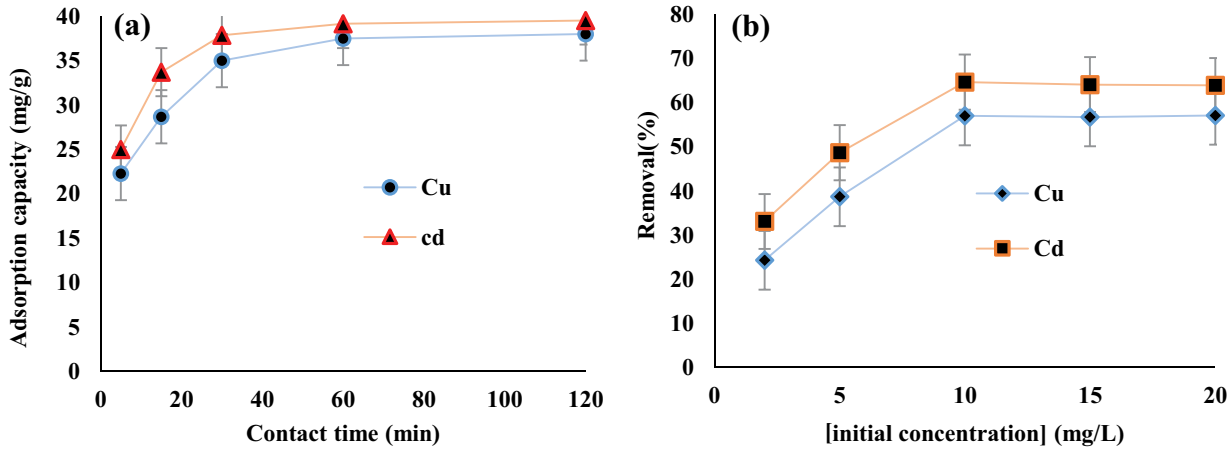

Fig. 6. Effect of contact time (a), and initial concentration (b) on the removal of heavy metals by Fe_3O_4@SiO_2-EDTA nanoparticles Cu^{2+} and Cd^{2+} = 5 mg/L, adsorbent dose: 0.1 g/L, time = 120 min and pH = 7.

Similar results have been reported in adsorption of Cu^{2+} and Cd^{2+} onto oil tea shell in water [16]. This event can be associated with the natural differences of Cu^{2+} and Cd^{2+} including their electro negativities (1.90 and 1.70, respectively), and their ionic radius (0.72 and 1.03 Å, respectively). Accordingly, lower adsorption tendency of the Fe_3O_4@SiO_2-EDTA particles toward Cd^{2+} than Cu^{2+} cations can be explained as its lower electronegativity [29].

3.7. Adsorption isotherms

Result of Langmuir constants in modeling the Fe_3O_4@SiO_2-EDTA has been presented in Table 3. With plotting C_e/q_e vs. C_e for Langmuir isotherm model in Fig. 7a, it appears that this isotherm model has a good coefficient of determination (R^2 = 0.9913) in fit of the adsorption process. As it can be seen in Table 3. Langmuir constants q_m, R_L, and K_a are as following: q_m = 79.4 for Cu^{2+} and 73.51 for Cd^{2+} (mg/g), R_L = 0.011 for Cu^{2+} and 0.014 for Cd^{2+}, and K_a = 0.75 for Cu^{2+} and 0.58 for Cd^{2+} (L/mg). In Table 4, a comparison of maximum adsorption capacity (q_m) of different adsorbents for Cu^{2+} and Cd^{2+} is prepared. As shown, Fe_3O_4@SiO_2-EDTA has a good q_m in comparison with other studies. Furthermore, R_L (dimensionless parameter that indicates the relative volatility in vapor–liquid equilibrium with a range between 0 and 1 for a favorable equilibrium [21]) is in the favorable range in this study. Therefore, it can be concluded that the adsorption of the metals onto the Fe_3O_4@SiO_2-EDTA had a good favorable equilibrium.

Table 3 shows the Freundlich isotherm model for adsorption of the metals onto the Fe_3O_4@SiO_2-EDTA. It appears that this isotherm model has a poor coefficient of determination (R^2 = 0.976) in fit of the adsorption process. As prepared in Table 3, the constants of Freundlich isotherm (K_f and n) are 48.42 for Cu^{2+} and 31.58 for Cd^{2+}, and 5.74 for Cu^{2+} and 3.79 for Cd^{2+}, respectively. High amount of K_f constant represents a very large extent of adsorption of the metals onto the Fe_3O_4@SiO_2-EDTA. Also, the value of n is larger than 1, which indicates a favorable adsorption

Table 3
Adsorption isotherm parameters of Cu^{+2} and Cd^{+2} onto Fe_3O_4@SiO_2-EDTA

Model	Parameter	Cu^{+2}	Cd^{+2}
Freundlich equation	K_f(L/mg)	48.426	31.58
	N	5.742	3.792
	R^2	0.976	0.974
Langmuir equation	q_m(mg/g)	79.4	73.51
	K_a(L/mg)	0.7521	0.589
	R_L	0.011	0.014
	R^2	0.9913	0.99

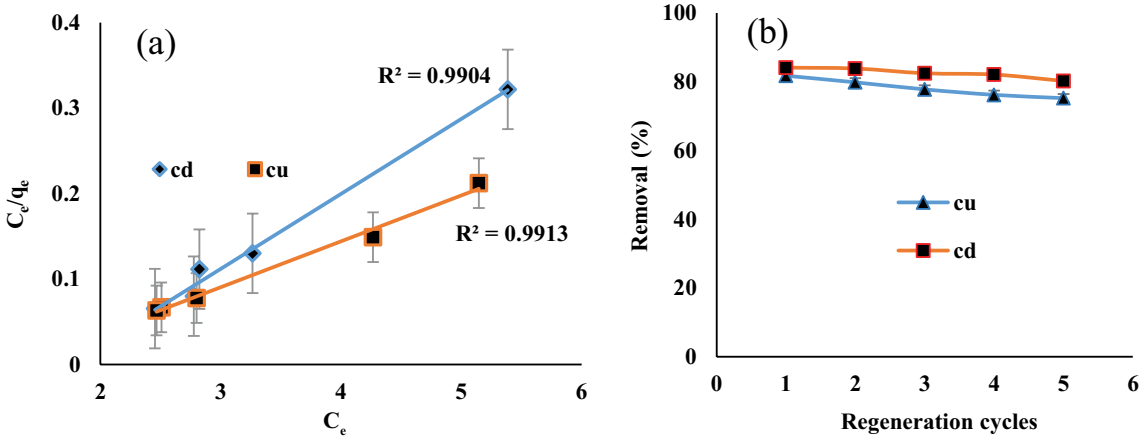

Fig. 7. Langmuir isotherm model (a), recovery from Fe_3O_4@SiO_2-EDTA (b).

Table 4
Comparison of maximum adsorption capacity (q_m) of different adsorbents for Cu^{+2} and Cd^{+2}

Adsorbent	Maximum adsorption capacity (mg/g)		Reference
	Cu^{+2}	Cd^{+2}	
TiO_2/SiO_2/Fe_3O_4 nanoparticles		670.9	[31]
Oil tea shell	12.1	14.2	[27]
EDTA functionalized magnetic nanoparticle		79.365	[29]
EDTA-functionalized silica spheres	37.59	23.67	[22]
Nanocomposites Fe_3O_4@SiO_2	0.58 mmol/g	0.45 mmol/g	[16]
Magnetic EDTA-modified chitosan/SiO_2/Fe_3O_4	0.495 mmol/g	0.040 mmol/g	[22]
Fe_3O_4@SiO_2-EDTA nano composite	79.4	73.51	This work

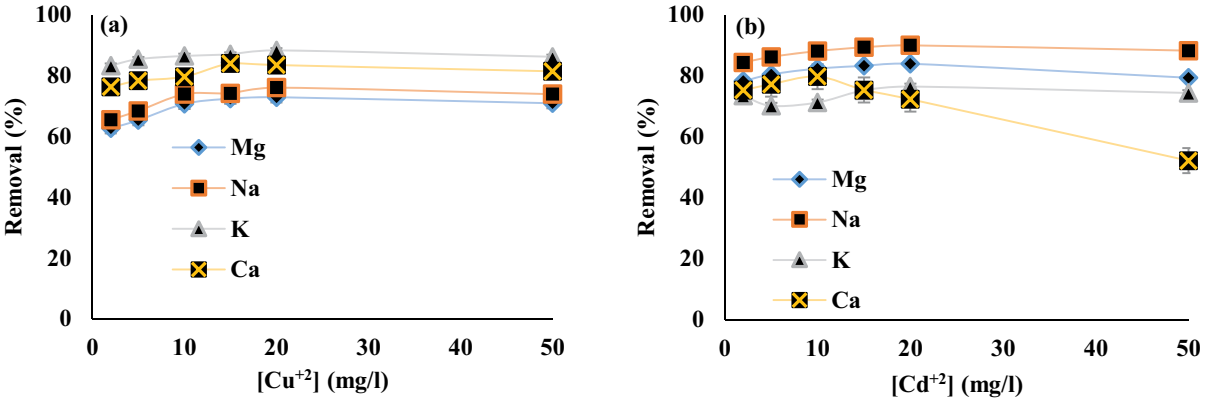

Fig. 8. Effect of various cations on (a) Cu^{2+} and (b) Cd^{2+}.

system and a multilayer physical process in the adsorption of the metals by the Fe_3O_4@SiO_2-EDTA [30,31].

3.8. Regeneration and reuse of Fe_3O_4@SiO_2-EDTA

Desorption is an important phenomenon that enables recycling of metal ions and adsorbents, which helps economic sustainability of adsorption-based treatment systems. According to a recent study, many chemicals can be applied as desorption agents. The agent should be selected carefully due to the permanent structural changes and adsorption capacity reductions that different chemicals can induce to adsorbent materials [27]. For this purpose, HCl (0.1 N) solution is used. As it can be seen in Fig. 7b, 80% of the Fe_3O_4@SiO_2-EDTA NPs can be recovered within five adsorption–desorption cycles without any significant loss of adsorption capacity.

3.9. Effect of disturbing cations on the adsorption process

As illustrated in Fig. 8, the presence of the Na^+, K^+, and Mg^{2+} metal ions does not have any inhibitory effect on adsorption of Cd^{2+} and Cu^{2+} onto Fe_3O_4@SiO_2-EDTA. However, the presence of Ca^{2+} decreases the capacity of Cu^{2+} adsorption. These findings are due to the stronger interaction and stable chemical bonding of Cd^{2+} and Cu^{2+} with the adsorbent relative to Na+, K^+, Cu^{2+}, and Mg^{2+}. According to the log K values of these ions (log K Cu^{2+} = 18.8, log K Cd^{2+} = 16.46, log K Na^+ = 1.7, log K Mg^{2+} = 8.7, log K Cu^{2+} = 10.69), Cu^{2+} can establish a more stable bond relative to the Na^+, K^+, and Mg^{2+} cations and the chemical bonding of Cd^{2+} is slightly weaker than that of Cu^{2+}. Therefore, among the four examined coexisting cations, Ca^{2+} has a better chance for competition with both Cd^{2+} and Cu^{2+} ions, and Cd^{2+} is more vulnerable to being affected by the competition [16,28]. Regardless of the competition, the coexisting cations do not considerably influence adsorption of Cu^{2+} and Cd^{2+} onto Fe_3O_4@SiO_2-EDTA.

4. Conclusion

In this study, we investigated the efficiency of Fe_3O_4@SiO_2 NPs modified with EDTA for adsorption of the Cu^{2+} and Cd^{2+} cations from aqueous solutions. According to the conducted evaluations, the adsorption efficiency of the cations enhances with the increase of adsorbent dose and contact time. However, our results show that the maximum adsorption efficiency of heavy metals is at pH = 7 with an initial concentration of Cu^{2+} and Cd^{2+} cations of 10 mg/g, an adsorbent dose of 0.1 g/L, and a contact time of 60 min. Studying isotherm models indicated that the adsorption process follows the Langmuir isotherm model. It means the adsorption process is homogenous and the adsorbed ions are mono-layered. Investigation of kinetic models suggested that the adsorption process follows pseudo-second-order kinetic model. Finally, a comparison between this study and other studies shows that the Fe_3O_4@SiO_2–EDTA has a high potential to remove Cu^{2+} and Cd^{2+} cations simultaneously from aqueous solution.

References

[1] L. Yang, T. Wen, L. Wang, T. Miki, H. Bai, X. Lu, H. Yu, T. Nagasaka, The stability of the compounds formed in the process of removal Pb(II), Cu(II) and Cd(II) by steelmaking slag in an acidic aqueous solution, J. Environ. Manage., 231 (2019) 41–48.
[2] Q. Yang, Z. Li, X. Lu, Q. Duan, L. Huang, J. Bi, A review of soil heavy metal pollution from industrial and agricultural regions in China: pollution and risk assessment, Sci. Total Environ., 642 (2018) 690–700.
[3] S. Sobhanardakani, R. Zandipak, Synthesis and application of TiO_2/SiO_2/Fe_3O_4 nanoparticles as novel adsorbent for removal of Cd(II), Hg(II) and Ni(II) ions from water samples, Clean Technol. Environ. Policy., 19 (2017) 1913–1925.
[4] R. V. Ferreira, I.L.S. Pereira, L.C.D. Cavalcante, L.F. Gamarra, S.M. Carneiro, E. Amaro, J.D. Fabris, R.Z. Domingues, A.L. Andrade, Synthesis and characterization of silica-coated nanoparticles of magnetite, Hyperfine Interact., 195 (2009) 265–274.
[5] A. Salido, B.T. Jones, Simultaneous determination of Cu, Cd and Pb in drinking-water using W- coil AAS, Talanta, 50 (1999) 649–659.
[6] L. Wang, L. Yang, Y. Li, Y. Zhang, X. Ma, Z. Ye, Study on adsorption mechanism of Pb(II) and Cu(II) in aqueous solution using PS-EDTA resin, Chem. Eng. J., 163 (2010) 364–372.
[7] N. Neyaz, M.S.S. Zarger, W.A. Siddiqui, Synthesis and characterisation of modified magnetite super paramagnetic nano composite for removal of toxic metals from ground water, Int. J. Environ. Sci., 5 (2014) 260–269.
[8] R. Zandipak, S. Sobhanardakani, Synthesis of $NiFe_2O_4$ nanoparticles for removal of anionic dyes from aqueous solution, Desal. Wat. Treat., 57 (2016) 11348–11360.
[9] X. Min, X. Wu, P. Shao, Z. Ren, L. Ding, X. Luo, Ultra-high capacity of lanthanum-doped UiO-66 for phosphate capture:

unusual doping of lanthanum by the reduction of coordination number, Chem. Eng. J., 358 (2019) 321–330.
[10] D. You, X. Min, L. Liu, Z. Ren, X. Xiao, S.G. Pavlostathis, J. Luo, X. Luo, New insight on the adsorption capacity of metallogels for antimonite and antimonate removal: from experimental to theoretical study, J. Hazard. Mater., 346 (2018) 218–225.
[11] S. Sobhanardakani, R. Zandipak, R. Sahraei, Removal of Janus Green dye from aqueous solutions using oxidized multi-walled carbon nanotubes, Toxicol. Environ. Chem., 95 (2013) 909–918.
[12] Z. Han, J. Li, X. Han, X. Ji, X. Zhao, A comparative study of iron-based PAN fibrous catalysts for peroxymonosulfate activation in decomposing organic contaminants, Chem. Eng. J., 358 (2019) 176–187.
[13] W.H.M. Abdelraheem, M.K. Patil, M.N. Nadagouda, D.D. Dionysiou, Hydrothermal synthesis of photoactive Nitrogen- and Boron- codoped TiO_2 nano-particles for the treatment of Bisphenol A in wastewater: synthesis, photocatalytic activity, degradation byproducts and reaction pathways, Applied Catal. B, (2018), doi: 10.1016/j.apcatb.2018.09.039.
[14] R. Zandipak, S. Sobhanardakani, Novel mesoporous Fe_3O_4/SiO_2/CTAB–SiO_2 as an effective adsorbent for the removal of amoxicillin and tetracycline from water, Clean Technol. Environ. Policy, 20 (2018) 871–885.
[15] E. Repo, T.A. Kurniawan, J.K. Warchol, M.E.T. Sillanpää, Removal of Co(II) and Ni(II) ions from contaminated water using silica gel functionalized with EDTA and/or DTPA as chelating agents, J. Hazard. Mater., 171 (2009) 1071–1080.
[16] Y. Liu, R. Fu, Y. Sun, X. Zhou, S.A. Baig, X. Xu, Multifunctional nanocomposites Fe_3O_4@SiO_2-EDTA for Pb(II) and Cu(II) removal from aqueous solutions, Appl. Surf. Sci., 369 (2016) 267–276.
[17] X. Zhao, Y. Shi, T. Wang, Y. Cai, G. Jiang, Preparation of silica-magnetite nanoparticle mixed hemimicelle sorbents for extraction of several typical phenolic compounds from environmental water samples, J. Chromatogr. A, 1188 (2008) 140–147.
[18] H. Sun, L. Cao, L. Lu, Magnetite/reduced graphene oxide nanocomposites: one step solvothermal synthesis and use as a novel platform for removal of dye pollutants, Nano Res., 4 (2011) 550–562.
[19] C. Zhao, L. Ma, J. You, F. Qu, R.D. Priestley, EDTA- and amine-functionalized graphene oxide as sorbents for Ni(II) removal, Desal. Wat. Treat., 57 (2016) 8942–8951.
[20] Y.F. Shen, J. Tang, Z.H. Nie, Y.D. Wang, Y. Ren, L. Zuo, Preparation and application of magnetic Fe_3O_4 nanoparticles for wastewater purification, Sep. Purif. Technol., 68 (2009) 312–319.
[21] N. Karapinar, R. Donat, Adsorption behaviour of Cu^{2+} and Cd^{2+} onto natural bentonite, Desalination, 249 (2009) 123–129.
[22] Y. Ren, H.A. Abbood, F. He, H. Peng, K. Huang, Magnetic EDTA-modified chitosan/SiO_2/Fe_3O_4 adsorbent: preparation, characterization, and application in heavy metal adsorption, Chem. Eng. J., 226 (2013) 300–311.
[23] R. Kumar, M.A. Barakat, Y.A. Daza, H.L. Woodcock, J.N. Kuhn, EDTA functionalized silica for removal of Cu(II), Zn(II) and Ni(II) from aqueous solution, J. Colloid Interface Sci., 408 (2013) 200–205.
[24] D. Naghipour, K. Taghavi, M. Moslemzadeh, Removal of methylene blue from aqueous solution by Artist's Bracket fungi: kinetic and equilibrium studies, Water Sci. Technol., 73 (2016) 2832–2840.
[25] Z. Li, B. Yu, H.L. Cong, X.-Y. Zhang, Q.-H. Peng, EDTA-modified DR/SiO_2 adsorbent: preparation, characterization, and application in heavy metal adsorption, Integr. Ferroelectr., 169 (2016) 1–6.
[26] S. Pourkarim, F. Ostovar, M. Mahdavianpour, M. Moslemzadeh, Adsorption of chromium(VI) from aqueous solution by Artist's Bracket fungi, Sep. Sci. Technol., 52 (2017) 1733–1741.
[27] D.Q. Melo, V.O.S. Neto, J.T. Oliveira, A.L. Barros, E.C.C. Gomes, G.S.C. Raulino, E. Longuinotti, R.F. Nascimento, Adsorption equilibria of Cu^{2+}, Zn^{2+}, and Cd^{2+} on EDTA-functionalized silica spheres, J. Chem. Eng. Data., 58 (2013) 798–806.
[28] Y. Huang, A.A. Keller, EDTA functionalized magnetic nanoparticle sorbents for cadmium and lead contaminated water treatment, Water Res., 80 (2015) 159–168.
[29] L. Cui, Y. Wang, L. Gao, L. Hu, L. Yan, Q. Wei, B. Du, EDTA functionalized magnetic graphene oxide for removal of Pb(II), Hg(II) and Cu(II) in water treatment: adsorption mechanism and separation property, Chem. Eng. J., 281 (2015) 1–10.
[30] O.R. Pal, A.K. Vanjara, Removal of malathion and butachlor from aqueous solution by clays and organoclays, Sep. Purif. Technol., 24 (2001) 167–172.
[31] J. Liu, C. Hu, Q. Huang, Adsorption of Cu^{2+}, Pb^{2+}, and Cd^{2+} onto oiltea shell from water, Bioresour. Technol., 271 (2019) 487–491.